Intense self-compressed, self-phase-stabilized few-cycle pulses at 2 μm from an optical filament

C. P. Hauri and R. B. Lopez-Martens

Laboratorie d'Optique Appliquée, ENSTA—Ecole Polytechnique, CNRS UMR 7639, F-91761 Palaiseau, France

C. I. Blaga,* K. D. Schultz,† J. Cryan, R. Chirla, P. Colosimo,* G. Doumy,* A. M. March,* C. Roedig, E. Sistrunk, J. Tate, J. Wheeler, and L. F. DiMauro

Department of Physics, Ohio State University, Columbus, Ohio 43210, USA

E. P. Power

Center for Ultrafast Optical Science, University of Michigan, Ann Arbor, Michigan 48109, USA

Received October 11, 2006; revised December 14, 2006; accepted January 4, 2007; posted January 8, 2007 (Doc. ID 75883); published March 5, 2007

We report the compression of intense, carrier-envelope phase stable mid-IR pulses down to few-cycle duration using an optical filament. A filament in xenon gas is formed by using self-phase stabilized 330 μJ 55 fs pulses at 2 μm produced via difference-frequency generation in a Ti:sapphire-pumped optical parametric amplifier. The ultrabroadband 2 μm carrier-wavelength output is self-compressed below 3 optical cycles and has a 270 μJ pulse energy. The self-locked phase offset of the 2 μm difference-frequency field is preserved after filamentation. This is to our knowledge the first experimental realization of pulse compression in optical filaments at mid-IR wavelengths ($\lambda > 0.8$ μm). © 2007 Optical Society of America

OCIS codes: 190.5530, 320.5520.

Progress in strong-field physics has been accelerated by the development of lasers operating near the 0.8 μm wavelength that feature high peak power, few-cycle duration, and reliable control over the carrier-envelope phase[1] (CEP). Furthermore, the fundamental scaling laws[2,3] governing the intense laser–atom interaction suggest that the advancement of longer-wavelength mid-IR laser sources capable of similar optical quality will have a major impact in strong-field physics. The most compelling examples include the generation of shorter attosecond x-ray bursts and the rescattering of electrons at kilovolt energies.[3–5]

A recently demonstrated 80 μJ, 2 μm prototype system[6] based on optical parametric chirped-pulse amplification via difference-frequency generation defines a standard for future development of long-wavelength drivers. However, the optical parametric chirped-pulse amplification architecture is faced with important technical challenges,[7] such as the need for specific pump laser design and unwanted generation of parasitic fluorescence underlying the primary pulse for high parametric gain configurations.[6]

Currently, femtosecond optical parametric amplifiers (OPAs) pumped by multimillijoule Ti:sapphire chirped-pulse amplification systems can deliver multicycle pulses in the mid-IR with sufficient peak power to investigate the efficacy of the nonlinear pulse compression techniques developed at shorter wavelengths. In particular, optical filaments formed in a noble gas by intense 0.8 μm pulses have demonstrated pulse compression down to the few-cycle regime with excellent beam stability and spatial mode quality.[8]

This Letter demonstrates, for the first time to our knowledge, the self-compression in an optical filament of high-peak-power mid-IR pulses derived by difference-frequency generation in a Ti:sapphire pumped OPA. This efficient scheme produces fluorescence-free, sub-3 optical cycle pulses near the 2 μm wavelength with 270 μJ energy at a 1 kHz repetition rate. The intense 2 μm field carries a constant CEP offset, thus making it an attractive long-wavelength driver for benchmark strong-field experiments.

A schematic of the experimental setup is shown in Fig. 1. High-peak-power multicycle mid-IR pulses are produced in a slightly modified traveling-wave OPA (TOPAS, Light Conversion) pumped by 4 mJ, 55 fs pulses from a home-built kilohertz Ti:sapphire amplifier operating at 0.81 μm. Initially, superfluorescence is generated in a β-barium borate (BBO) crystal pumped by a small fraction of the Ti:sapphire light. The same crystal also acts as a subsequent preamplifier of the signal beam (~1.3 μm). Finally, a 2 mm long BBO crystal, which acts as a power amplifier, is synchronously seeded by the amplified signal and the

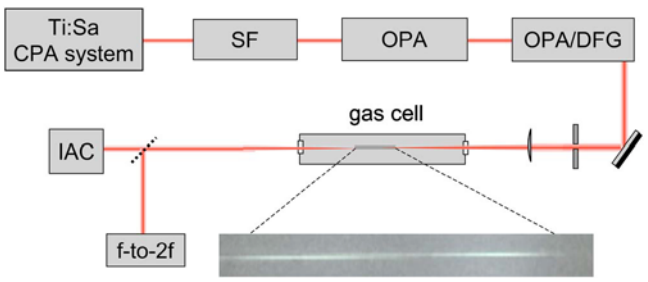

Fig. 1. (Color online) Mid-IR filament pulse compression setup, showing superfluorescence generator (SF), dual-stage OPA, gas cell for filamentation and diagnostics. Inset, fluorescence from a xenon filament. DFG, difference-frequency generation; IAC, interferometric autocorrelator.

0146-9592/07/070868-3/$15.00

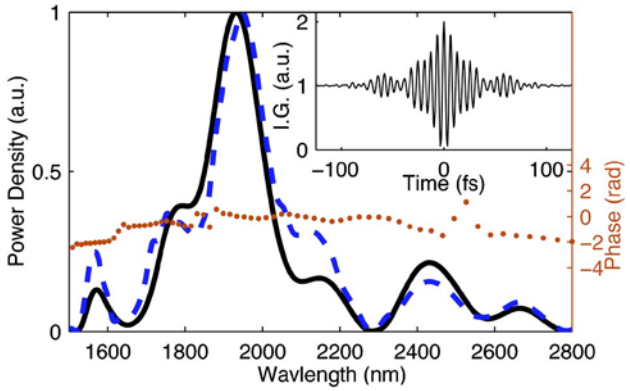

Fig. 2. (Color online) Measured interferogram (inset), resulting power spectrum (solid black), best-fit power spectrum (dashed blue), and best-fit spectral phase (dotted red).

remaining 0.81 μm pump beam, yielding 500 μJ of 2 μm light. The final amplifier's noncollinear geometry allows spatial separation of pump, signal, and idler beams, thereby eliminating the need for spectral filtering.

Our OPA scheme provides two crucial elements. First, passive synchronization produces an intrinsically small temporal jitter between signal and pump pulses, thus resulting in exquisite pulse-to-pulse stability. Second, since both the pump and the signal fields originate from the same coherent source, the CEP offset of the generated mid-IR idler field is constant for consecutive pulses[9–11] despite the absence of any active stabilization of the pump laser. The 50 nm (FWHM) OPA output spectrum at 2 μm is consistent with the 55 fs pump pulse duration. Once focused, the pulses can reach the threshold for self-focusing and therefore warrant nonlinear spectral broadening and pulse compression via filamentation.

An optical filament is produced by weakly focusing the mid-IR light with an 0.5 m focal length spherical mirror into a 1 m long cell filled with xenon (2.15×10^5 Pa). Filamentary propagation is verified by recording the plasma fluorescence (Fig. 1) and reveals the presence of two consecutive nonlinear focusing–defocusing cycles within the roughly 10 cm long filament. Segments with strong fluorescence emission (brightest regions in the photograph) imply regions with larger ionization and therefore higher intensities. Initially, the strong self-focused beam (first section) is mediated by the equally strong defocusing of the plasma electrons. This results in a lowering of the intensity and thus a reduction in fluorescence before self-focusing starts another focusing–defocusing cycle. Finally, diffraction terminates both nonlinear propagation and spectral broadening. However, during propagation through the filament the beam undergoes extreme spectral broadening, emerging with an octave of bandwidth (solid curve, Fig. 2).

In addition to the spectral broadening, the self-guided beam undergoes significant spatial mode shaping during filamentation. This results in an improvement of the intrinsically poor beam quality of the idler, yielding better focusing for high-field applications.

Temporal characterization of the ultrabroadband mid-IR pulses was performed using an interferometric autocorrelation (IAC) technique. 2 μm thick pellicle with a broadband coating at 2 μm acts as a 50/50 beam splitter in a Michelson interferometer. As shown in the inset in Fig. 2, an interferogram was recorded by using the linear response of an InGaAs photodiode, and the resulting spectrum is also shown in the figure. The pulse duration is measured by using a second-order autocorrelator based on a two-photon-induced photocurrent[12] from a saturated InGaAs diode and is shown in Fig. 3. The pulse is reconstructed from the measured spectrum and second-order autocorrelation by the PICASO method[13] with an adaptive genetic algorithm[14] as our functional minimization routine. Briefly, the PICASO method seeks the optimum spectral phase to minimize the rms error Δ between the measured autocorrelation and the autocorrelation from the reconstructed pulse. Due to shot-to-shot power fluctuations in the OPA's output (±5% rms), the self-phase-modulation-broadened spectrum is expected to reflect the variations in power. Consequently, the measured interferogram and autocorrelation contains a source of noise that cannot be removed with simple frequency-domain filters. To retrieve an improved fit to the measured autocorrelation, we parameterized the spectral power, in addition to the spectral phase, using the initial interferogram-derived power spectrum as a baseline and bounding the search space to exclude the consideration of unreasonable spectra. Figure 2 displays the best-fit power spectrum and spectral phase; the fit deviates from the measured second-order autocorrelation by an rms error of $\Delta = 0.062$, as shown in Fig. 3. The inset in Fig. 3 shows that the retrieved pulse has a FWHM duration of 17.9 fs, while the frequency spectrum supports a 12.2 fs transform-limited pulse. The absence of any external compression elements suggests that the pulse is self-compressed during filamentation. In fact, the (negative) dispersion of the cell exit window (1.5 mm thick CaF_2) compensates for the (positive) dispersion introduced by propaga-

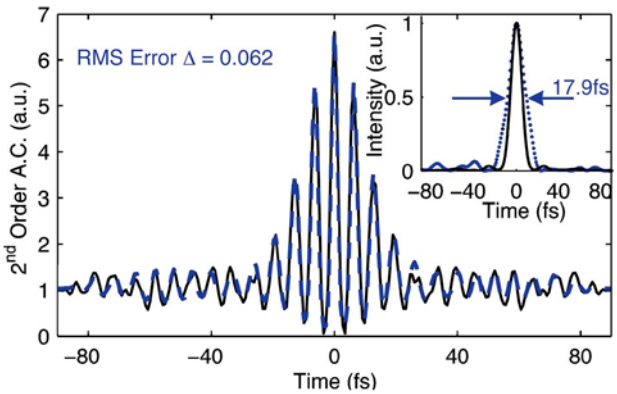

Fig. 3. (Color online) Measured second-order autocorrelation (solid) and best-fit second-order autocorrelation (dashed). Inset, transform-limited intensity profile (solid) and best-fit intensity profile (dashed). The reduced fringe contrast ratio for the second-order autocorrelation trace is due to beam pointing instabilities.

tion in air (2 m), preserving the few-cycle pulse shape in our autocorrelator.

Characterization of the CEP stability after the filament was measured by using a *f*-to-2*f* spectral interferometer. In contrast to other CEP measurements, no additional white-light generation was required, since the filament generates an octave-spanning spectrum. A 0.5 mm thick BBO crystal was used to frequency double the central portion of the fundamental spectrum, which interfered with the blue side of the ultrabroadband white light near 0.9 μm. Figure 4(a) plots a series of high-contrast interferograms (each trace integrated over 10 ms) as a function of time and shows excellent fringe stability for 8800 consecutive shots, while Fig. 4(b) shows an averaged interferogram trace over a 120 s. The residual rms CEP drift is smaller than 0.1 rad, which is unexpected for an OPA seeded by fluorescence.[9] However, the measurement clearly shows that not only is the CEP offset preserved through propagation but also that the filament dynamics is conducive to long-term stability. Similar measurements have been performed using the signal ($\lambda = 1.3$ μm) for driving filamentation. In this configuration the CEP offset was measured to be random. We therefore conclude that filamentation does not stabilize but only preserves the CEP offset.

In conclusion we have demonstrated the use of self-guided filamentation for spectral broadening and pulse compression of a mid-IR pulse. The pulse originating from an optical parametric amplifier is artificially broadened in a xenon cell, producing a 17 fs, 0.27 mJ pulse at 2 μm. The high peak power, good spatial beam profile, and excellent CEP stability preserved during filamentary propagation provides an attractive source for investigating strong-field physics at mid-IR wavelengths.

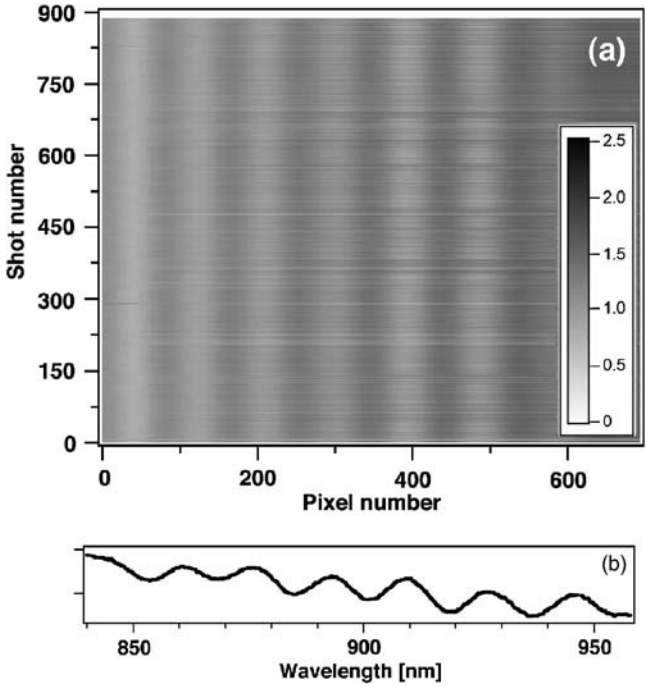

Fig. 4. (a) Time series of *f*-to-2*f* interferograms acquired for 8,800 consecutive laser shots. Each individual interference pattern was integrated over 10 ms (10 shots). (b) Fringe pattern integrated over 12×10^4 consecutive laser shots (120 s).

The authors thank S. Dhillon from Thales Research and Technology for providing the GaAs substrates. This work was performed with support from the U.S. Department of Energy Office of Basic Energy Sciences under contract DE-FG-02-04ER15614 and the National Science Foundation under contract GRT962706. We also acknowledge additional support from the Chaire d'Excellence program of the French Agence Nationale pour la Recherche (ANR) and the Hagenlocker Chair endowment. C. P. Hauri's e-mail address is hauri@ensta.fr.

*Permanent address, Department of Physics, Stony Brook University, Stony Brook, New York 11794, USA.

†Present address, Department of Physics, Austin Peay State University, Clarksville, Tennesse 37044, USA.

References

1. A. Baltuska, T. Udem, M. Uiberacker, M. Hentschel, E. Goulielmakis, C. Gohle, R. Holzwarth, V. S. Yakovlev, A. Scrinzi, T. W. Haensch, and F. Krausz, Nature **421**, 611 (2003).
2. L. V. Keldysh, Sov. Phys. JETP **20**, 1307 (1965).
3. J. Tate, T. Auguste, H. G. Muller, P. Salieres, P. Agostini, and L. F. DiMauro, Phys. Rev. Lett. **98**, 013901 (2007).
4. A. Gordon and F. X. Kaertner, Opt. Express **13**, 2941 (2005).
5. P. Agostini and L. F. DiMauro, Rev. Roum. Phys. **67**, 813 (2004).
6. T. Fuji, N. Ishii, C. Y. Teisset, X. Gu, Th. Metzger, A. Baltuska, N. Forget, D. Kaplan, A. Galvanauskas, and F. Krausz, Opt. Lett. **31**, 1103 (2006).
7. A. Dubietis, R. Butkus, and A. P. Piskarkas, IEEE J. Sel. Topics Quantum Electron. **12**, 163 (2006).
8. C. P. Hauri, W. Kornelis, F. W. Helbing, A. Heinrich, A. Couairon, A. Mysyrowicz, J. Biegert, and U. Keller, Appl. Phys. B **79**, 673 (2004).
9. A. Baltuska, T. Fuji, and T. Kobayashi, Phys. Rev. Lett. **88**, 133901 (2002).
10. T. Fuji, A. Apolonski, and F. Krausz, Opt. Lett. **29**, 632 (2004).
11. C. Manzoni, G. Cerullo, and S. De Silvestri, Opt. Lett. **29**, 2668 (2004).
12. J. K. Ranka, A. L. Gaeta, A. Baltuska, M. S. Pshenichnikov, and D. A. Wiersma, Opt. Lett. **22**, 1344 (1997).
13. J. W. Nicholson and W. Rudolph, J. Opt. Soc. Am. B **19**, 330 (2000).
14. B. J. Pearson, J. L. White, T. C. Weinacht, and P. H. Bucksbaum, Phys. Rev. A **63**, 063412 (2002).